Reviews

Crystal Structure Determination from Powder Diffraction Data

Kenneth D. M. Harris*

School of Chemistry, University of Birmingham, Edgbaston, Birmingham B15 2TT, U.K.

Maryjane Tremayne

Department of Chemistry, University College London, 20 Gordon Street, London WC1H 0AJ, U.K.

Received April 8, 1996. Revised Manuscript Received August 15, 1996[⊗]

A wide range of important crystalline solids cannot be prepared in the form of single crystals of suitable size and quality for structural characterization by conventional single-crystal X-ray diffraction methods. The development of techniques for crystal structure determination from *powder* diffraction data is clearly important for allowing the structural characterization of such materials. Although the structure refinement stage of the structure determination process can now be carried out fairly routinely using the Rietveld profile refinement technique, structure solution directly from powder diffraction data is associated with several intrinsic difficulties. The article surveys the field of crystal structure determination from powder diffraction data. Particular emphasis is given to the challenging structure solution stage of the structure determination process, with illustrative case studies highlighting the features of each of the main methods that are currently used for structure solution from powder diffraction data. The current scope and future potential of powder diffraction as an approach for crystal structure determination are discussed, and contemporary applications of this approach across several disciplines within materials chemistry are reviewed.

1. Introduction

X-ray diffraction is undoubtedly the most important and powerful technique for characterizing the structural properties of crystalline solids. Single-crystal X-ray diffraction, in particular, is now used widely and routinely for crystal structure determination. However, many important crystalline solids cannot be prepared as single crystals of sufficient size and quality for conventional single-crystal X-ray diffraction studies, and in such cases it is essential that structural information can be determined from powder diffraction data. In this review, we focus on the application of powder diffraction to determine information on the structural properties of crystalline solids.

Crystal structure determination from diffraction data can be divided into three stages: (1) determination of lattice parameters and assignment of crystal symmetry and space group, (2) structure solution, and (3) structure refinement. In structure solution, an initial structural model is derived directly from the experimental diffraction data. If this initial structural model is a sufficiently good representation of the true structure, refinement of this model against the experimental diffraction data can be carried out to obtain a good-quality crystal structure. For single-crystal diffraction data, both structure solution and structure refinement calculations can now generally be carried out in a straightforward manner. For powder diffraction data, on the other hand, refinement of crystal structures (usually carried out using the Rietveld profile refinement technique[1]) can now be carried out fairly routinely, whereas solution of crystal structures directly from powder diffraction data is a significantly greater challenge. The field of crystal structure solution from powder diffraction data is currently an active area of research, both in the development of new and more powerful methodologies and improved instrumentation and in the application of existing techniques to tackle problems of increasing complexity. As described below, significant progress has been made in recent years in all aspects of this field.

We now consider in more detail the difficulties associated with solving crystal structures directly from powder diffraction data. Essentially the same information is contained in single-crystal and powder diffraction patterns, but in the former case this information is distributed in three-dimensional space whereas in the latter case the three-dimensional diffraction data are "compressed" into one dimension. As a consequence, there is generally considerable overlap of peaks in the powder diffraction pattern, leading to severe ambiguities in extracting the intensities $I(hkl)$ of individual diffraction maxima. Despite this fact, the traditional approach for crystal structure solution from powder

* To whom correspondence should be addressed.
⊗ Abstract published in *Advance ACS Abstracts,* October 1, 1996.

S0897-4756(96)00218-9 CCC: $12.00

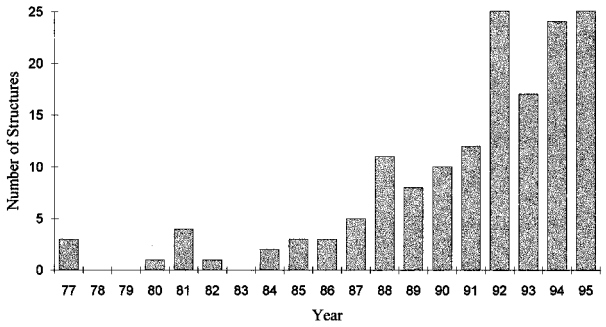

Figure 1. Number of previously unknown crystal structures solved since 1977 from X-ray and neutron powder diffraction data.

diffraction data is to attempt to extract the intensities $I(hkl)$ of individual reflections directly from the powder diffraction pattern and then to use these $I(hkl)$ data in the types of crystal structure solution technique (e.g., direct methods and the Patterson method) that are used for single-crystal diffraction data. The major difficulty with this approach arises in extracting values of $I(hkl)$ that are sufficiently reliable to lead to a successful structure solution calculation. This problem of extensive peak overlap in the powder diffraction pattern limits the complexity of structures that can be solved successfully by such methods. As a consequence, sophisticated methods are now being developed to improve the reliability of extracting intensity information for such overlapping peaks. Virtually all the techniques for structure solution from powder diffraction data (including the Patterson method, direct methods, and the method of entropy maximization and likelihood ranking, discussed in sections 5.1−5.3, respectively) consider values of $I(hkl)$ extracted from the powder diffraction pattern, and, despite the difficulties that this entails, these approaches are nevertheless the most widely used at the present time.

An alternative philosophy for crystal structure solution from powder diffraction data is to postulate structural models independently of the powder diffraction data, with the suitability of these models assessed by direct comparison of the powder diffraction patterns calculated for these models against the experimental powder diffraction pattern. This comparison is quantified using the profile R factor (as used in Rietveld refinement), which considers the whole digitized intensity profile (not the integrated intensities of individual diffraction maxima) and therefore implicitly takes care of the overlap of peaks. This approach avoids the problematic step of extracting values of $I(hkl)$ from the powder diffraction pattern; no partitioning of the experimental powder diffraction profile into a set of "single-crystal-like" intensities $I(hkl)$ is carried out, and the avoidance of such partitioning of the data is an important strength of this approach. This philosophy is embodied within the Monte Carlo and simulated annealing methods, which are discussed in section 5.4.

Although considerable progress has been made in recent years[2−8] (see Figure 1), the solution of crystal structures from powder diffraction data is still far from routine, and there is still considerable potential for the continued development and improvement of the methodologies in this field. The aim of this review is to survey the current scope and limitations of crystal structure determination from powder diffraction data, with particular emphasis on the structure solution stage of the structure determination process. Here we focus on the use of the Patterson method, direct methods, the method of entropy maximization and likelihood ranking, and Monte Carlo and simulated annealing methods for structure solution, although we note that other approaches (including grid searches, energy minimization calculations, and other computer simulation techniques for structure prediction) have also been used. After giving an overview of the methods presently available for crystal structure determination from powder diffraction data, the application of these methods across a wide range of disciplines within materials chemistry is reviewed.

2. Radiation Sources

Although a great deal of work on crystal structure determination from powder diffraction data has made use of conventional laboratory X-ray diffractometers, there are significant advantages in using synchrotron X-ray diffraction data over laboratory data. The combination of high brightness and good vertical collimation of synchrotron X-radiation can be fully exploited in the construction of diffractometers that give data with substantially improved signal/noise ratio and higher resolution. With high resolution, the problem of peak overlap is substantially alleviated, allowing a greater amount of unambiguous intensity information to be extracted from the powder diffraction pattern and sometimes enabling successful determination of the lattice parameters in cases for which this is not possible with laboratory X-ray powder diffraction data. Furthermore, the tunability of synchrotron radiation sources allows the X-ray wavelength to be changed readily, and this can be exploited to diminish the effects of X-ray absorption or to give insights into the positions and site occupancies of atoms of a specific type (by studying the differences between powder diffraction patterns recorded for wavelengths on either side of an absorption edge for the selected type of atom[5]).

Although it is clearly preferable to use synchrotron X-ray powder diffraction data for structure determination, the use of synchrotron data is generally not essential; this is a consequence of the continued improvements in the resolution and sensitivity of laboratory X-ray powder diffractometers (allowing data of sufficiently high quality to be recorded[9]) and advances in the methodology for structure determination. Clearly the opportunity to determine crystal structures reliably from X-ray powder diffraction data collected on laboratory diffractometers is opening up the field to a much wider community of users.

The vast majority of crystal structure determinations are carried out using X-ray diffraction data, but in certain circumstances it may be advantageous to use neutron diffraction data. One important difference between neutron and X-ray diffraction is that the relative scattering powers of atoms for neutrons and X-rays are significantly different. In the case of X-ray diffraction, the scattering power increases monotonically with atomic number and hence light atoms, such as hydrogen, are weak X-ray scatterers. Neutrons, on the other hand, are scattered by atomic nuclei, and neutron-scattering power varies irregularly across the periodic table (hence atoms with similar atomic number, even

isotopes of the same element, may have significantly different neutron-scattering properties). Another important difference is that interference effects cause X-ray scattering by an atom to diminish with increasing scattering angle, whereas the scattering of neutrons by an atom is essentially isotropic. As a consequence, a neutron powder diffraction pattern contains significantly more intensity information, particularly at high diffraction angle, than the X-ray powder diffraction pattern of the same material.

A small number of structures have been determined directly from neutron powder diffraction data (examples are given in refs 10−14), although in most cases it is easier to solve a structure from X-ray powder diffraction data rather than neutron powder diffraction data. With X-ray data, it is often sufficient to locate only a small subset of the atoms (usually the strongest scatterers) during the structure solution stage, with the remainder of the atoms located subsequently in the structure refinement stage (by application of difference Fourier techniques). With neutron data, on the other hand, it is usually necessary to locate the majority of the atoms during the structure solution stage, in order for subsequent structure refinement to be successful. For these reasons, a good approach is to solve as much of the structure as possible from X-ray data and to use neutron data subsequently to locate light atoms or to distinguish between atoms that have similar X-ray scattering powers. A joint Rietveld refinement can then be carried out using the X-ray and neutron diffraction data, leading to a crystal structure determination of improved quality. Illustrative examples of such joint refinements are given in refs 15−18 and emphasize the complementary nature of X-ray and neutron diffraction techniques.

The subsequent discussion in this article is focused on the use of X-ray powder diffraction data (both from synchrotron and conventional laboratory sources) for crystal structure solution, although all the methods discussed are applicable to both X-ray and neutron powder diffraction data. In section 5, the application of each structure solution technique is illustrated by a detailed example; all of these examples refer to the use of X-ray powder diffraction data measured using a conventional laboratory diffractometer.

3. Phase Problem in Crystal Structure Solution

In the diffraction pattern from a crystalline solid, the diffraction maximum with Miller indexes (hkl) is characterized by the scattering vector $\boldsymbol{h}$ in reciprocal space, with $\boldsymbol{h} = h\boldsymbol{a}^* + k\boldsymbol{b}^* + l\boldsymbol{c}^*$ ($\boldsymbol{a}^*$, $\boldsymbol{b}^*$, and $\boldsymbol{c}^*$ denote the reciprocal lattice vectors). The scattering for reflection $\boldsymbol{h}$ is completely defined by the structure factor $F(\boldsymbol{h})$ which has amplitude $|F(\boldsymbol{h})|$ and phase $\alpha(\boldsymbol{h})$ and is related to the electron density $\rho(\boldsymbol{r})$ within the unit cell by

$$F(\boldsymbol{h}) = |F(\boldsymbol{h})| \exp(i\alpha(\boldsymbol{h})) = \int \rho(\boldsymbol{r}) \exp[2\pi i \boldsymbol{h}\cdot\boldsymbol{r}]\, \mathrm{d}\boldsymbol{r} \quad (1)$$

where $\boldsymbol{r}$ is the vector $\boldsymbol{r} = x\boldsymbol{a} + y\boldsymbol{b} + z\boldsymbol{c}$ in direct space ($\boldsymbol{a}$, $\boldsymbol{b}$, and $\boldsymbol{c}$ denote the direct lattice vectors) and integration is over all vectors $\boldsymbol{r}$ in the unit cell. From eq 1, it follows that

$$\rho(\boldsymbol{r}) = (1/V)\sum_{h} |F(\boldsymbol{h})| \exp[i\alpha(\boldsymbol{h}) - 2\pi i \boldsymbol{h}\cdot\boldsymbol{r}] \quad (2)$$

where V denotes the volume of the unit cell, and the summation is over all vectors $\boldsymbol{h}$ with integer coefficients h, k, and l. If the values of both $|F(\boldsymbol{h})|$ and $\alpha(\boldsymbol{h})$ could be measured directly from the diffraction pattern, then $\rho(\boldsymbol{r})$ (i.e., the "crystal structure") could be determined directly from eq 2 by summing over the measured reflections $\boldsymbol{h}$ (note that this would only be an approximation to $\rho(\boldsymbol{r})$, as only a finite set of reflections $\boldsymbol{h}$ is actually measured experimentally). However, while the values of $|F(\boldsymbol{h})|$ can be obtained experimentally (they are related to the measured diffraction intensities $I(\boldsymbol{h})$), the values of $\alpha(\boldsymbol{h})$ cannot be determined directly from the experimental diffraction pattern. This constitutes the so-called "phase problem" in crystallography. To solve the crystal structure, it is clearly necessary to have methods that provide an estimate of the values of the phases $\alpha(\boldsymbol{h})$ that should be combined with the experimentally derived values of $|F(\boldsymbol{h})|$.

4. Preliminary Stages of Structure Determination

4.1. Determination of Lattice Parameters and Space Group Assignment. An essential prerequisite for crystal structure determination is that the lattice parameters and the space group are known. Determination of the lattice parameters from the powder diffraction pattern requires accurate determination of the peak positions (i.e., accurate d-spacing data), which can normally be achieved using a peak-search process, provided all systematic errors have been eliminated (e.g., by careful measurement of the zero-point error in the position of the detector). Although in favorable cases the lattice parameters can be determined from first principles (generally feasible only for high-symmetry structures), it is usually necessary to use an "autoindexing" program such as ITO,[19] TREOR,[20] or DICVOL.[21]. These programs adopt different approaches,[22] and it is valuable to have more than one program available since experience shows that the relative successes of different autoindexing programs can differ from one set of powder diffraction data to another. In general, the autoindexing programs generate several possible sets of lattice parameters that are consistent, to a greater or lesser degree, with the set of measured peak positions; a variety of figures of merit[23,24] can be used to rank the proposed sets of lattice parameters.

The space group is assigned by identifying the conditions for systematic absences in the indexed powder diffraction data. If it is not possible to assign the space group uniquely, it may be necessary to carry out the structure solution calculation in parallel for several different plausible space groups.

4.2. Extraction of Diffraction Intensities from the Powder Diffraction Pattern. In the conventional approach (adopted in the Patterson method, direct methods and the maximum entropy method) for crystal structure solution from powder diffraction data, the intensities ($I(\boldsymbol{h})$) of individual diffraction maxima are extracted from the experimental powder diffraction pattern. In the ideal case, each peak in the powder diffractogram would be individually resolved, and it would then be straightforward to extract accurate values of $I(\boldsymbol{h})$. However, extraction of intensities from the powder diffractogram is complicated by the overlap

of nonequivalent reflections due to (1) "accidental" equality (or near-equality) of d spacings for nonequivalent reflections, especially at high scattering angle (this can be particularly severe for low-symmetry structures), or (2) symmetry-imposed equality of d spacings for well-defined groups of nonequivalent reflections [this occurs only for high-symmetry structures; e.g., for reflections $\{hkl\}$ and $\{khl\}$ in a tetragonal system with Laue group $4/m$, $d(hkl) = d(khl)$ but $I(hkl) \neq I(khl)$].

In early work in this field, peaks that overlap significantly were commonly ignored or assigned arbitrary (often equal) contributions to the total intensity of the overlapping set. However, this approach is clearly unsatisfactory, and more sophisticated approaches for determining reliable relative intensities from overlapping peaks have been developed. The most commonly used of these "pattern decomposition" techniques are based on the use of Rietveld profile fitting procedures (see section 6.2) in which the whole powder diffraction pattern is decomposed in one step. These techniques adopt a least-squares approach to fit a calculated profile to the experimental powder diffraction pattern (without the use of a structural model) by refinement of the lattice parameters, the zero-point error, peak-shape parameters, and parameters defining the background. Integrated peak intensities can then be determined from the fitted profile. The seminal work in this field was carried out by Pawley,[25] with particular reference to neutron powder diffraction data. Specific developments of the method for use with X-ray powder diffraction data (for which the 2θ dependence and asymmetry of the peak shape require more detailed consideration) have been addressed by Toraya.[26] Another widely used profile-fitting procedure is that of Le Bail,[27] in which problems arising from negative intensities in the Pawley method are overcome. These pattern decomposition techniques are incorporated in a number of programs, including ALLHKL,[25] WPPF,[26] GSAS,[28] FULLPROF,[29] LSQPROF,[30] PROFIL,[31] and EXTRA.[32]

As most approaches for structure solution from powder diffraction data depend heavily on extracting reliable intensity information, pattern decomposition constitutes an important step dictating the overall success of these approaches. Inevitably, however, the intensities determined for overlapping peaks by pattern decomposition contain inherent uncertainties, particularly when the positions of the peaks in the overlapping set are separated by less than half the half-width of the peaks. Approaches are currently being developed to allow the relative intensities of such overlapping peaks to be determined accurately and include the application of relations between the structure factors derived from direct methods and the Patterson function (DOREES[33]), an iterative procedure involving the calculation of a squared Patterson map and subsequent back-transformation giving a new set of structure factors for the overlapping reflections (FIPS[34]), a method based on entropy maximization of a Patterson function,[35,36] and a Bayesian fitting procedure.[37]

5. Crystal Structure Solution from Powder Diffraction Data

5.1. Patterson Method. *5.1.1. Method.* The Patterson function[38]

$$P(\boldsymbol{r}) = (1/V)\sum_{h}|F(\boldsymbol{h})|^2 \exp[-2\pi i \boldsymbol{h}\cdot\boldsymbol{r}] \qquad (3)$$

uses only the observed structure factor amplitudes $|F(\boldsymbol{h})|$ (determined from the measured diffraction intensities $I(\boldsymbol{h})$) and does not require information on the phases of reflections. Each peak in the Patterson map $P(\boldsymbol{r})$ corresponds to an interatomic vector $(\boldsymbol{r}_i - \boldsymbol{r}_j)$ within the unit cell, with the height of each peak proportional to the product of the scattering powers of the atoms i and j. In principle, the positions of atoms in the unit cell can be deduced from the set of interatomic vectors represented in the Patterson map. If the structure contains a small number of atoms that scatter significantly more strongly than the others, the interatomic vectors between these atoms dominate the Patterson map, allowing the positions $(\boldsymbol{r}_j)$ of these atoms to be deduced readily. For many cases of this type, the Patterson method has been used successfully for structure solution from X-ray powder diffraction data (examples are given in refs 16, 18, and 39−44). Unfortunately, if the structure does not contain a small number of dominant scatterers, the Patterson map is densely packed with peaks of comparable intensity, from which it may be difficult or impossible to derive a reliable interpretation of the positions of the atoms in the unit cell.

The Patterson function may also be used to determine the position of a structural fragment of well-defined geometry (e.g., a rigid group), even if this fragment does not contain a dominant scatterer. This interpretation of the Patterson function arises because a structural fragment of well-defined geometry gives rise to a well-defined set of interatomic vectors which will be represented by a characteristic set of peaks in the Patterson map; thus, a knowledge of molecular geometry is exploited in this structure solution approach. In many cases, the fragment search process is applied in Patterson space and is usually divided into two parts, as follows.

(1) A rotation search to determine the orientation of the fragment. A vector model is constructed from the known geometry of the fragment, superimposed on the Patterson map, and rotated into all possible orientations until the optimum fit with the Patterson map is found.

(2) A translation search to determine the position of the oriented fragment within the unit cell. This involves translation of the correctly oriented fragment into all possible positions in the asymmetric unit. The interatomic vectors corresponding to each position of the fragment are then calculated and compared with the Patterson map derived from the experimental data to find the position corresponding to the best fit.

Similar procedures have also been applied to fragment searches operating in reciprocal space (PATMET[45]) and in a combination of direct space and reciprocal space (ROTSEARCH[46]). Patterson search routines have also been incorporated into direct methods programs (PATSEE[47]). These model-based Patterson methods have been used (PATMET,[48,49] ROTSEARCH,[50,51] PATSEE[52]) to solve the crystal structures of molecular materials from X-ray powder diffraction data.

The number of intensity measurements $I(\boldsymbol{h})$ required for successful structure solution by the Patterson method is usually somewhat smaller than for direct methods (see section 5.2), and it may therefore be possible to

reduce the number of overlapping peaks considered in the Patterson calculation (by truncating the experimental data at a maximum value of 2θ that is lower than that required for direct methods). Furthermore, the Patterson method is often able to derive reasonable structural information from diffraction data that are inferior in quality to that required for successful structure solution by direct methods. These features make the Patterson method an attractive choice for structure solution from powder diffraction data, provided the structure is known to contain a small number of dominant scatterers or a structural fragment of well-defined geometry.

5.1.2. Example. We now illustrate the application of the Patterson method to determine the previously unknown structure of anhydrous lithium perchlorate ($LiClO_4$) from X-ray powder diffraction data (step size $\Delta 2\theta = 0.02°$; total data collection time = 3 h).[95] The powder diffraction pattern was indexed using the program TREOR, on the basis of the first 20 observable reflections, producing the following unit cell: $a = 8.651$ Å, $b = 6.913$ Å, $c = 4.829$ Å, $\alpha = \beta = \gamma = 90°$ (with figures of merit $M_{20} = 44$, $F_{20} = 39$ (0.007 843, 66)). The system was assigned as orthorhombic, with systematic absences consistent with space groups *Pnma* (centrosymmetric) and $Pn2_1a$ (noncentrosymmetric). Structure solution was initially attempted in the centrosymmetric space group *Pnma*. Integrated intensities were extracted from the powder diffraction pattern in two ranges ($10° < 2\theta < 40°$ and $35° < 2\theta < 75°$) using the Le Bail profile-fitting procedure. The data from these two regions were then combined to give a set of 84 reflections and were then used to generate a Patterson map, from which the position of the Cl atom was clearly evident. After Rietveld refinement of the position of the Cl atom, a difference Fourier synthesis revealed the positions of all three O atoms in the asymmetric unit. Subsequent refinement of these positions and further difference Fourier synthesis identified the position of the Li atom. The final Rietveld refinement of the complete structure converged to $R_{wp} = 10.60\%$, $R_p = 8.32\%$, $R_F = 11.10\%$, $R_B = 9.21\%$, and $\chi^2 = 1.53$ for 28 variables and 3250 profile points in the range $10° < 2\theta < 75°$ (84 reflections) [note: a general discussion of Rietveld refinement is given in section 6.2 and includes definitions of these agreement factors]. The experimental and calculated X-ray powder diffraction patterns, and the corresponding difference profile, are shown in Figure 2. The position of the Cl atom found from the Patterson map was close (0.54 Å) to the position of this atom in the final refined structure.

The final refined fractional coordinates and isotropic atomic displacement parameters for $LiClO_4$ are given in Table 1. As shown in Figure 3, there is a distorted octahedral arrangement of O atoms surrounding each Li atom. All bond lengths and bond angles in the refined structure are within acceptable limits consistent with the precision of the data [Cl−O bond lengths 1.43(1)−1.46(1) Å; O−Cl−O bond angles 108(1)−111(1)°; Li−O distances 1.98(1)−2.40(1) Å]. It is relevant to note that both the accuracy and the precision of these structural parameters would be improved with the combined use of X-ray and neutron powder diffraction data in a joint refinement.

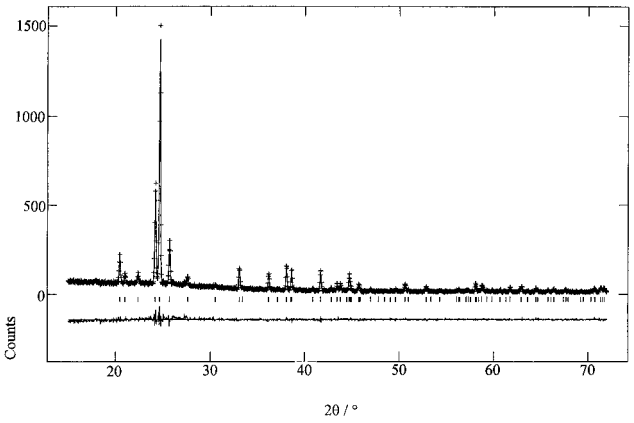

Figure 2. Experimental (+), calculated (solid line), and difference (below) powder diffraction profiles for the Rietveld refinement of $LiClO_4$. Reflection positions are marked.

Table 1. Final Atomic Coordinates and Isotropic Atomic Displacement Parameters Obtained from the Rietveld Refinement Calculation for $LiClO_4$[a]

atom	site type	*x/a*	*y/b*	*z/c*	U_{iso}/Å^2
Cl	4c	0.318(4)	1/4	0.543(8)	0.025(2)
O1	4c	0.149(1)	1/4	0.546(2)	0.020(3)
O2	8d	0.370(1)	0.079(1)	0.681(1)	0.021(2)
O3	4c	0.374(1)	1/4	0.261(2)	0.031(3)
Li	4b	1/2	0	0	0.069(9)

[a] *Pnma*; $a = 8.6522(4)$ Å, $b = 6.9152(3)$ Å, $c = 4.8299(2)$ Å.

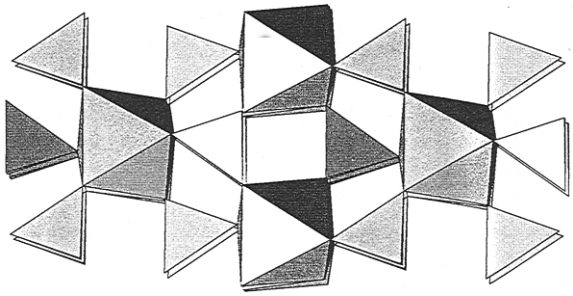

Figure 3. Final refined crystal structure of $LiClO_4$ showing the octahedral coordination of ClO_4^- tetrahedra around each Li atom.

5.2. Direct Methods. *5.2.1. Method.* The term "direct methods" describes a class of statistical methods that attempt to derive knowledge of the phases $\alpha(\boldsymbol{h})$ directly from the measured diffraction intensities $I(\boldsymbol{h})$. The direct methods approach is based on the fact that the observed structure factor amplitudes $|F(\boldsymbol{h})|$ (determined from $I(\boldsymbol{h})$), together with the correct (but initially unknown) values of $\alpha(\boldsymbol{h})$, must correspond (via eq 2) to an electron density that is positive everywhere within the unit cell. This imposes constraints on $\alpha(\boldsymbol{h})$, and by applying probability relationships, the probable phases ($\alpha_p(\boldsymbol{h})$) of well-defined groups of reflections can be deduced. The positions of atoms in the initial structural model are then usually obtained from an E-map, constructed using the trial phases $\alpha_p(\boldsymbol{h})$ as follows:

$$\chi(\boldsymbol{r}) = (1/V)\sum_{\mathbf{h}}|\mathrm{E}(\boldsymbol{h})| \exp[i\alpha_p(\boldsymbol{h}) - 2\pi i\boldsymbol{h}\cdot\boldsymbol{r}] \quad (4)$$

where $|\mathrm{E}(\boldsymbol{h})|$ are normalized structure factors (calculated from $|F(\boldsymbol{h})|$). All aspects of the direct methods procedure for crystal structure solution are discussed in refs 53 and 54.

The direct methods approach has become the most widely used technique for structure solution from

powder diffraction data. Unlike the Patterson method, the direct methods approach does not rely on the presence of a dominant scatterer or prior knowledge of the geometry of a well-defined structural fragment, and, in principle, it can be applied to a much greater variety of structural problems. Although weak reflections can often be omitted from the data used in structure solution by Patterson methods, this is not advisable for direct methods. These reflections play an important role in the direct methods calculation, and their absence would lead to errors in the normalization and phasing processes and in the calculation of some figures of merit used to discriminate between the correct structure solution and incorrect structure solutions. A significant number of such weak reflections in a powder diffractogram are present as overlapping peaks, and the fact that the intensities assigned to these reflections are often unreliable may lead to problems in the phasing process.

Until recently, the application of direct methods to powder diffraction data was carried out using programs developed for single-crystal diffraction data (for example MULTAN,[55] SHELXS,[56] MITHRIL,[57,58] SIR,[59,60] SIMPEL[61]). However, direct methods procedures optimized for powder diffraction data have now been developed (SIRPOW,[60,62] SIMPEL[63]). For example, in the case of SIRPOW, knowledge of the number of reflections in each group of overlapping reflections and the total intensity of each group are required. Initially, the individual reflections within each group are assigned equal intensities, and these intensities are then modified during the calculation as more phase information is obtained. The use of reliable intensities (importantly for weak reflections) strengthens the process of phase determination and improves the ability of the figures of merit to discriminate the correct structure solution.

Examples of the successful application of direct methods in structure solution from powder diffraction data are given in refs 44 and 64−71.

5.2.2. Example. As an example of the application of direct methods to crystal structure solution from powder diffraction data, we highlight the structure determination of *p*-methoxybenzoic acid ($CH_3OC_6H_4CO_2H$). This is an "equal-atom" system (see section 8.2.2), the structure of which was already known from single-crystal X-ray diffraction[72] (monoclinic, $P2_1/a$; $a = 16.968$ Å, $b = 10.962$ Å, $c = 3.968$ Å, $\beta = 98.13°$). For the structure solution from X-ray powder diffraction data, individual intensities were extracted from the diffractogram in two ranges ($7.5° < 2\theta < 35°$ and $35° < 2\theta < 75°$) using the Le Bail profile-fitting procedure. These data ranges were then combined to generate a total set of 372 reflections (169 nonoverlapping and 203 overlapping, according to a visually judged criterion ($\Delta 2\theta \approx 0.05°$)) which were used in the direct methods program SIRPOW. However, the resulting solution showed only two clear peaks (and no identifiable molecular fragment) in the E-map, and subsequent attempts to complete and refine this structure were unsuccessful. Closer examination of the powder diffraction pattern showed a high degree of overlap for $2\theta > 70°$, so a subsequent direct methods calculation was carried out using only the intensity data in the range $7.5° < 2\theta < 70°$ (306 reflections; 162 nonoverlapping and 144 overlapping). Although no molecular fragment could be recognized readily from the E-map, six peaks slightly higher than the rest were used as an initial model for structure refinement. The remaining non-hydrogen atoms were located using difference Fourier analysis, and the complete structure was refined, with the application of geometric restraints, by the Rietveld refinement technique. No attempt was made to determine the positions of the H atoms.

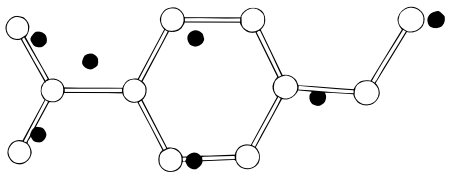

Figure 4. Atomic positions (filled circles) determined from the direct methods structure solution calculation for *p*-methoxybenzoic acid compared with the molecular structure (open circles) in the final refined crystal structure.

In Figure 4, the atomic positions established from the direct methods calculation are compared with the corresponding positions in the final refined crystal structure (the distances between corresponding atoms were in the range 0.44−0.89 Å). Although the model taken from the structure solution stage comprised only six atoms, it was clear in retrospect (in comparison with the final structure) that the direct methods calculation had actually located a further O atom.

5.3. Method of Entropy Maximization and Likelihood Ranking. *5.3.1. Method.* The maximum entropy technique is a powerful method of image reconstruction and has been applied successfully in a wide range of scientific fields.[73−75] In crystallography, the maximum entropy criterion has been used to examine the crystallographic inversion problem,[76] to generate high-quality electron density maps,[77,78] as a means of partitioning the intensities of completely overlapping reflections in powder diffraction patterns,[35,36] and as an approach for direct phase determination.[79−82] Recently, a technique for crystal structure solution, in which phases are determined on the basis of entropy maximization and likelihood ranking,[83] has been developed and applied successfully to single-crystal X-ray diffraction data,[84] protein diffraction data,[85] and electron microscopy data.[86,87] As now described, this method has also been used in crystal structure solution from X-ray powder diffraction data.[15,88−91]

The maximum entropy and likelihood method adopts a similar approach to conventional direct methods for phase determination. Both methods consider an unknown crystal structure to be composed of atoms of known identity but unknown positions. Initially, these positions are considered as random with a uniform distribution in the asymmetric unit. The structure solution process consists of the gradual removal of this randomness. In its application to powder diffraction data, the maximum entropy and likelihood method handles groups of overlapping peaks in a rational manner, enabling intensity information for these peaks to be used productively in the structure solution process. The procedure for structure solution from powder diffraction data using the maximum entropy and likelihood method (implemented in the program MICE[84]) is now summarized.

First, the peaks in the powder diffraction pattern are divided into two sets, according to whether they are nonoverlapping or overlapping. For each overlapping

group of reflections, the intensities of the individual reflections are summed to give a combined intensity for the group. Both sets of reflections are then normalized to give unitary structure factors.

The origin is defined by fixing the phases of an appropriate number of reflections, chosen from the set of nonoverlapping reflections and satisfying the usual rules and criteria.[54] These reflections constitute the initial basis set. As described below, the basis set is subsequently extended in the course of the structure solution process by incorporating new reflections. Thus, a "phasing tree" is constructed, with each addition of new reflections defining a successive level of this tree.

The known phases of the reflections in the basis set are used as the constraints in an entropy maximization procedure that gives rise to phase extrapolation. Specifically, a maximum entropy map is constructed, and the Fourier transform of this map produces new intensity and phase information for reflections not in the basis set (while also reproducing the amplitudes and phases of the basis set reflections used to generate the map). However, when the basis set comprises only the origin-defining reflections, the extrapolated intensities and phases are not reliable. This situation is improved successively at each level of the phasing tree by incorporating new phase information into the basis set with the addition of selected strong reflections. The phases of these reflections are taken as 0 or π for centrosymmetric structures and $+\pi/4$, $-\pi/4$, $+3\pi/4$ or $-3\pi/4$ for noncentrosymmetric structures (thus guaranteeing that each trial phase must be within $\pi/4$ of the correct phase). In adding new reflections to the basis set, all permutations of the phases of these new reflections are considered. The addition of new reflections with permuted phases represents the next level of the phasing tree, with each possible permutation of phases representing a different node within this level. Each node is subjected to constrained entropy maximization, thus updating the corresponding maximum entropy map.

At each level of the phasing tree, the most promising nodes are identified using the likelihood function, which evaluates the agreement between the structure factor amplitudes extrapolated from the maximum entropy map for the node and those from the experimental data. Thus, the likelihood function indicates the extent to which the experimentally determined (unphased) intensities are rendered more likely by the phase choices made for the basis set reflections for the node in question, than under the initial assumption of a uniform distribution. The use of overlapping reflections in the calculation of the likelihood greatly increases the ability to discriminate the optimum node. The nodes are ranked in order of log-likelihood gain (LLG)[88] and the LLG values are then analyzed for phase indications using the Student *t* test.[90] Application of the Student *t* test removes any inherent subjectivity that would be introduced in selecting nodes on the basis of likelihood alone. The most promising nodes are then retained, and the next level of the phasing tree is constructed by adding new reflections with permuted phases.

The phasing procedure and development of successive levels of the phasing tree are continued until most structure factors have significant phase indications or until the centroid map[92] reveals a recognizable structural model. The maximum entropy distribution associated with a node is not a traditional electron density map. To generate a map from which positions of atoms can be determined, the maximum entropy map is used to calculate a centroid map in which the weights involve normalized structure factors but the coefficients are unitary structure factors. Both basis set and non-basis set reflections are used to calculate the centroid map, and it is important to emphasize that the inclusion of overlapping reflections in this calculation generates a centroid map that is significantly clearer than that generated with the overlapping reflections excluded.

Recent developments in the maximum entropy and likelihood method include the use of a more efficient scheme for sampling permutations of trial phases based on error-correcting codes,[93] the use of envelopes in forbidden zones,[94] and the use of a fragment recycling procedure[92] in which a known fragment position is used actively in the structure solution calculation[95] (as illustrated in section 5.3.3).

5.3.2. Example 1. The combined maximum entropy and likelihood ranking technique has been applied to determine a previously unknown molecular crystal structure, *p*-toluenesulfonhydrazide ($CH_3C_6H_4SO_2NHNH_2$), from X-ray powder diffraction data.[89] The X-ray powder diffractogram was indexed using the program TREOR on the basis of the first 26 observable reflections, producing the following unit cell: $a = 18.568$ Å, $b = 5.630$ Å, $c = 8.524$ Å, $\alpha = \gamma = 90°$, $\beta = 106.2°$ (with figures of merit $M_{26} = 26$, $F_{26} = 56$ (0.009 830, 46)). The system was assigned as monoclinic, and systematic absences identified the space group unambiguously as $P2_1/n$. Integrated intensities were extracted from the powder diffraction pattern in two ranges ($7.5° < 2\theta < 40°$ and $35° < 2\theta < 65°$) using the Le Bail profile-fitting procedure. The data from these two regions were then combined, generating the intensities of 175 reflections, of which 93 were assigned as nonoverlapping and 82 were assigned as overlapping according to a visually judged criterion ($\Delta 2\theta \approx 0.05°$). The overlapping reflections were present in 34 groups, with a maximum of four reflections in each group, and the intensities in each group were combined to give an effective intensity for the group. Both the overlapping and nonoverlapping data were entered into the direct methods program MITHRIL to generate unitary structure factors. These were used as input for the maximum entropy and likelihood program MICE. The origin-defining reflections obtained from MITHRIL were used as the initial basis set, with phases of 0 assigned to these reflections. A further five reflections were selected and added to the basis set; the phases (0 or π) of these five reflections were permuted to generate 32 nodes. Entropy maximization was carried out on each node, and the log-likelihood gain (LLG) was calculated in each case. From analysis of the LLG values of these nodes using the Student *t* test at the 10% significance level, four nodes were retained for further consideration. The basis set was then expanded by adding four new reflections with permuted phases, thus generating 64 nodes (i.e., 4×2^4) in the second level of the phasing tree. Note that the resolution of all reflections used to enlarge the basis set was higher than 1.78 Å. Subsequent analysis allowed all but 16 nodes to be rejected; of these 16 nodes, four had significantly higher LLG (2.18 (node 44), 2.38 (node 52), 2.73 (node 80), and 2.61 (node 88)) than the

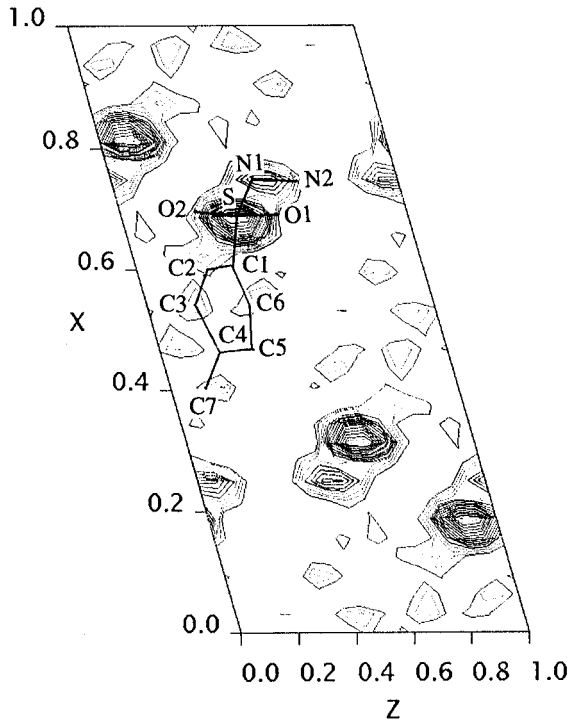

Figure 5. Centroid map, viewed in projection along the *b* axis, for node 52 in the structure solution calculation of *p*-$CH_3C_6H_4SO_2NHNH_2$ by the maximum entropy and likelihood ranking method. For comparison, the final refined position of the molecule is overlayed on the centroid map.

others (the next highest LLG was 1.52). From the centroid maps constructed for each node, it was clear that nodes 44 and 52 were almost identical, and nodes 80 and 88 were almost identical, and therefore only nodes 52 and 80 (the nodes of highest LLG in each pair) were studied further. The centroid map for node 52 contained two well-defined peaks with one of higher intensity than the other, whereas the centroid map for node 80 contained two well-defined peaks of similar intensity. The peaks from both nodes were used (as S and N atoms) as starting structural models for Rietveld refinement calculations. The refinement based on node 80 did not proceed satisfactorily, and only the refinement based on node 52 was pursued further. This was perhaps expected, as only node 52 displayed a dominant peak (corresponding to the S atom) in the centroid map.

The remaining C, O, and N atoms were located from difference Fourier calculations (no attempt was made to locate the H atoms). In the Rietveld refinement, isotropic atomic displacement parameters were constrained according to atom type. The final Rietveld refinement gave agreement factors $R_{wp} = 7.83\%$, $R_p = 5.95\%$, $R_F = 12.38\%$, $R_B = 9.59\%$, and $\chi^2 = 5.57$ for 59 variables and 3624 profile points in the range $7.5° < 2\theta < 80°$ (523 reflections). Retrospective examination of the centroid map corresponding to node 52 (as shown in Figure 5) revealed that four C atoms were evident in addition to the S and N atoms discussed above. Indeed, of the top seven peaks in the map, six corresponded to the positions of atoms in the final refined structure (the distances between these peaks and the corresponding atomic positions were in the range 0.33−0.82 Å).

5.3.3. Example 2. We now consider a second example involving the application of the maximum entropy and likelihood method to determine the crystal structure of lithium zirconate ($Li_6Zr_2O_7$). This example demonstrates the fragment recycling procedure and the use of codes in constructing the phasing tree. The crystal structure of lithium zirconate was originally solved from X-ray powder diffraction data using Patterson methods and refined using a combination of X-ray and neutron powder diffraction data.[16] In the work presented here, only the X-ray powder diffraction data were used. The structure is monoclinic (space group *C*2/*c*), with $a = 10.442$ Å, $b = 5.988$ Å, $c = 10.201$ Å, $\beta = 100.26°$. A total of 257 integrated intensities were extracted from the powder diffraction pattern over the range $5° < 2\theta < 90°$ using the Le Bail procedure. Of these reflections, 148 were assigned as nonoverlapping and 109 were assigned as overlapping, according to a visually judged criterion ($\Delta 2\theta \approx 0.05°$). The overlapping reflections were present in 47 groups, with a maximum of six reflections in each group, and for each group a combined intensity was considered. Both the overlapping and nonoverlapping data were entered into the direct methods program MITHRIL to generate unitary structure factors. These unitary structure factors were then used in the maximum entropy and likelihood program MICE. As before, the root node was created by assigning phases to two origin-defining reflections chosen by MITHRIL. A further seven reflections were added to the basis set, and their phases were permuted using a Hadamard code to give 16 nodes. Entropy maximization was carried out on each node, and the LLG was calculated in each case. The best eight nodes were retained, and the second phasing level was constructed by permutation (using the Hadamard code) of seven additional reflections on each of these nodes, generating a further 128 nodes. After entropy maximization of these nodes, the solutions corresponding to several of the best (i.e., highest likelihood) phase sets were inspected. The likelihood value of the best solution (node 135) was much higher than that of the next best solution, and the centroid map generated from node 135 showed a very dominant peak which was assigned as the zirconium atom.

MITHRIL was then used to process the additional information given by the recycling fragment (the zirconium atom) and to renormalize the data for use in MICE. In the recycling procedure, an arbitrary origin is not selected because the origin is already defined by the fragment, hence there is no root node. Five reflections were entered as the basis set and used to generate 32 nodes. Entropy maximization was then carried out on each node in the usual way, and both the LLG and NS+L values were calculated in each case (NS+L[83] is a good joint indicator of maximum entropy and maximum likelihood). One node clearly had the best LLG and NS+L values, and the centroid map generated from this node revealed the positions of all seven remaining atoms (Figure 6). These atomic positions were then refined to within experimental error of the published structure. In Table 2, the atomic positions obtained from the maximum entropy and likelihood recycling calculation are compared with the coordinates of the corresponding atoms in the known structure (refined using only the X-ray diffraction data).

For lithium zirconate, it is straightforward to locate the zirconium atom by Patterson methods and then to complete the structure using difference Fourier techniques. However, for cases in which the position of a

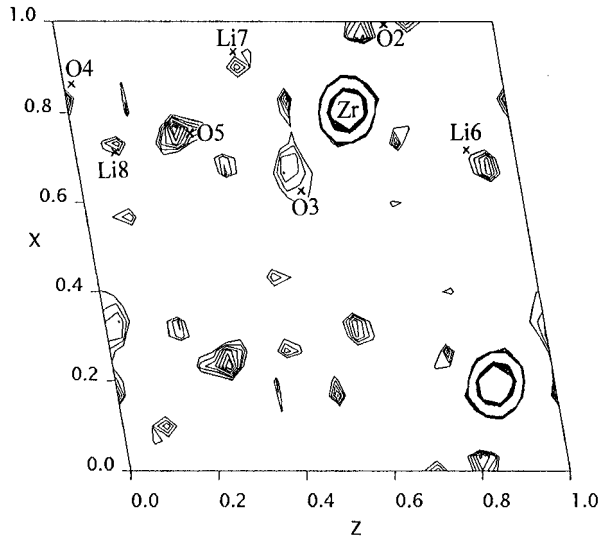

Figure 6. Centroid map, viewed in projection along the *b* axis, for the optimum node obtained from the recycling procedure for $Li_6Zr_2O_7$. For comparison, the final refined atomic positions are overlayed on the centroid map.

Table 2. Atomic Coordinates in the Structure Solution of $Li_6Zr_2O_7$ Obtained from the MICE Fragment Recycling Calculation (Second Line) and the Corresponding Coordinates Obtained in the Final Rietveld Refinement Using the X-ray Powder Diffraction Data (First Line)[a]

atom	site type	*x/a*	*y/b*	*z/c*	Δ/Å
Zr	8f	0.1822	0.1228	0.3640	
		0.1938	0.1223	0.3658	0.12
O5	8f	0.2552	0.3996	0.2594	
		0.2570	0.4340	0.2365	0.31
O4	8f	0.3786	0.3750	0.0208	
		0.3309	0.5009	−0.0033	0.91
O2	4e	0.0000	0.1252	0.2500	
		0.0168	0.1119	0.3023	0.54
Li6	8f	0.2993	0.1173	0.1128	
		0.3227	0.1115	0.0760	0.48
O3	8f	0.1335	0.3644	0.5067	
		0.1630	0.3702	0.4791	0.45
Li7	8f	0.4304	0.3947	0.3982	
		0.4014	0.3267	0.4003	0.51
Li8	8f	0.0614	0.3496	0.0972	
		0.0678	0.3840	0.0961	0.22

[a] For each atom, the parameter Δ represents the distance between the position in the structure solution and the corresponding position in the final refined structure. *C*2/*c*; $a = 10.4421(1)$ Å, $b = 5.9877(1)$ Å, $c = 10.2008(1)$ Å, $\beta = 100.255(1)°$. Atoms are listed in order of decreasing peak height in the centroid map.

strong scatterer is not a sufficient starting model for successful completion of the structure by difference Fourier techniques, it is clearly essential that more structural information can be obtained at the structure solution stage. The application of the fragment recycling procedure discussed in this example is likely to have a major impact in such cases.

5.4. Monte Carlo and Simulated Annealing Methods. *5.4.1. Method.* Monte Carlo methods[96−98] and the related simulated annealing approach[99,100] have been employed in many fields of science including electronics, biology, materials science, and image processing. More recently, these techniques have been developed and applied to crystal structure solution from X-ray powder diffraction data.[101−107] A similar approach, called the "reverse Monte Carlo" method, has been applied successfully to determine the structural properties of amorphous materials by fitting structural models to X-ray scattering and neutron-scattering data.[108,109]

The Monte Carlo method differs considerably from the traditional approaches for crystal structure solution from powder diffraction data, in that it operates in direct space (rather than reciprocal space or Patterson space). In particular, rather than extracting the intensities of individual diffraction maxima directly from the powder diffraction pattern, the strategy is to postulate structural models independently of the diffraction data. This involves the generation of a series of structural models $\{x_i: i = 1, ..., N\}$ by random movement of an appropriate collection of atoms (the so-called "structural fragment") within the unit cell, with the acceptance or rejection of each trial structure based (using the Metropolis importance sampling technique[110]) on the agreement between the experimental powder diffractogram and the powder diffractogram calculated for the trial structure. This agreement between the calculated and experimental diffraction data is assessed using the weighted profile *R* factor (R_{wp}, defined in section 6.2) calculated over the whole powder diffraction profile. From the large number of structures generated in the Monte Carlo calculation, the best structure is selected as the initial structural model for subsequent structure refinement.

The first structure (x_1) is generally chosen as a random position of the structural fragment in the unit cell. A series of structures is then generated, with each new structure not produced "from scratch" but derived from the previous structure. The process for generating structure x_{i+1} from structure x_i (termed a "Monte Carlo move") is as follows.

(1) Starting from structure x_i, the structural fragment is subjected to a random "displacement" to generate a trial structure x_{trial}. The exact form of this "displacement" depends on the type of structural fragment and may be constrained depending on symmetry and other structural considerations. In general, the displacement will consist of one or more of the following: (a) translation of the structural fragment by a random amount (subject to a user-specified maximum displacement) in a random direction; (b) rotation of the structural fragment by a random amount (subject to a user-specified maximum rotation angle) about a randomly chosen axis passing through the center of the structural fragment; (c) in the case of nonrigid structural fragments, random displacements (again subject to user-specified maximum values) in the values of internal degrees of freedom (e.g., torsion angles). The powder diffractogram corresponding to the trial structure is then calculated, and the scale factor is optimized using a least-squares fit of the calculated diffraction pattern to the experimental diffraction pattern (essentially a Rietveld refinement calculation in which only the scale factor is refined). The agreement factor for the trial structure is denoted $R_{wp}(x_{trial})$.

(2) The trial structure is then accepted or rejected on the basis of the difference *Z* between the value of R_{wp} for the trial structure and the value of R_{wp} for structure x_i [i.e., $Z = R_{wp}(x_{trial}) - R_{wp}(x_i)$]. If $Z \leq 0$, the trial structure is accepted as the new structure (i.e., $x_{i+1} = x_{trial}$). If $Z > 0$, however, the trial structure is accepted as the new structure (i.e., $x_{i+1} = x_{trial}$) with probability $\exp(-Z/S)$ and rejected with probability $[1 - \exp(-Z/S)]$, where *S* represents an appropriate scaling of *Z*, and operates in a manner analogous to kT in conventional Monte Carlo simulation techniques.[97,98] If

the trial structure is rejected, the new structure is taken to be the same as the previous structure (i.e., $x_{i+1} = x_i$).

Stages 1 and 2 are repeated to generate a Markov chain of structures x_{i+2}, x_{i+3}, x_{i+4}, ..., x_N. The maximum displacements of the structural fragment and the value of S are chosen so that the optimum proportion (ca. 40%) of trial moves is accepted,[111] giving rise to maximum efficiency in the propagation of the Monte Carlo algorithm. After a sufficiently extensive range of structural space has been explored by the structural fragment, the structure corresponding to lowest R_{wp} is considered as the starting structural model for Rietveld refinement. In many cases, the structural fragment considered in the Monte Carlo calculation is only a portion of the complete structure, and further development of the structure is therefore required through difference Fourier calculations.

As discussed in section 1, a major advantage of the Monte Carlo technique over the conventional methods of structure solution is that it does not directly extract structural information from the powder diffraction pattern, and hence the problem of extracting the intensities of individual reflections from overlapping groups is implicitly avoided.

It is important to emphasize that the Monte Carlo method does not involve minimization of R_{wp} (except in the case of $S = 0$) but explores structural space in a manner that gives emphasis to regions associated with low R_{wp}, with the ability to escape from local minima in R_{wp}. On the other hand, alternative approaches based on minimization of R_{wp} would generally locate a local minimum in R_{wp} close to the starting structure, rather than the global minimum in R_{wp}.

The main factor limiting the efficiency of the Monte Carlo calculation is the number of structural "degrees of freedom" varied during the calculation. For this reason the method is significantly more efficient when the structural fragment can be defined by a geometrically well-defined (rigid) group of atoms in which only the position and orientation of the structural fragment are varied in the Monte Carlo calculation. In many cases, however, it may be necessary to define a flexible structural fragment, requiring the variation of internal degrees of freedom (e.g., torsion angles), with corresponding demands in terms of computational time. Thus, in the assessment of the efficiency and feasibility of the Monte Carlo approach, the number of degrees of freedom in the structural fragment is, in general, a more important consideration than the number of atoms in the asymmetric unit.

The simulated annealing technique also uses the Monte Carlo algorithm to generate a series of structures, with each trial structure accepted or rejected using Metropolis importance sampling. However, the fundamental difference between the simulated annealing approach and the Monte Carlo method described above concerns the way in which the parameter S is handled. The simulated annealing approach can be considered as the application of the Metropolis algorithm at systematically decreasing values of S (analogous to decrease of temperature) under the control of an appropriate "annealing schedule". The initial value of S is chosen so that virtually all trial structures are accepted, and as S is decreased, the number of trial structures that are accepted decreases until the best structure solution is obtained. The final structure is then used as a starting structural model for Rietveld refinement. In the Monte Carlo method, on the other hand, the parameter S is generally fixed throughout the calculation so that the optimum proportion of trial structures is accepted, with the best structure solution identified by subsequent inspection of the series of structures generated. Nevertheless, it may be desirable to alter the value of S during the Monte Carlo calculation (for example, to encourage the structural fragment to explore a wider range of structural space, or to explore selected regions of structural space in more detail).

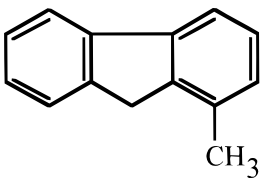

Figure 7. Structural formula of 1-methylfluorene.

The Monte Carlo technique has been applied to determine a number of crystal structures from X-ray powder diffraction data, involving different ways of handling the structural fragment. These include the following:

(1) Translation of a single dominant X-ray scatterer through the unit cell.[95]

(2) Independent translation of two dominant X-ray scatterers through the unit cell.[95]

(3) Rotation of a rigid structural fragment around a crystallographic center of symmetry.[105]

(4) Two separate Monte Carlo calculations involving (i) in the first calculation, location of a dominant scatterer by translation of this atom within the unit cell, and (ii) then, after establishing the correct position of the dominant scatterer, rotation of a rigid fragment around the fixed position of the dominant scatterer found in the first calculation.[103]

(5) Simultaneous translation and rotation of a rigid structural fragment within the unit cell.[106,107]

(6) Simultaneous translation and rotation of a flexible structural fragment within the unit cell, together with variation of intramolecular degrees of freedom.[112]

5.4.2. Example. We illustrate the application of the Monte Carlo approach for crystal structure solution from powder diffraction data by describing our determination of the previously unknown structure of 1-methylfluorene[107] ($C_{14}H_{12}$, Figure 7).

The X-ray powder diffraction pattern was indexed using the program TREOR, on the basis of the first 23 observable reflections, producing the following unit cell: $a = 14.278$ Å, $b = 5.691$ Å, $c = 12.362$ Å, $\alpha = \gamma = 90°$, $\beta = 95.1°$ (with figures of merit $M_{23} = 29$, $F_{23} = 59$ (0.007 047, 56)). The system was assigned as monoclinic, and systematic absences allowed the space group to be identified unambiguously as $P2_1/n$. The structural fragment used in the Monte Carlo calculation comprised the non-hydrogen atoms in the planar fluorenyl (C_{13}) group fixed at a geometry consistent with other derivatives of fluorene. Although the methyl carbon atom could readily have been included in the structural fragment, omission of this atom leads to a more efficient propagation of the Monte Carlo process as there is twice the probability of locating the structural fragment successfully [i.e., a structural fragment comprising the

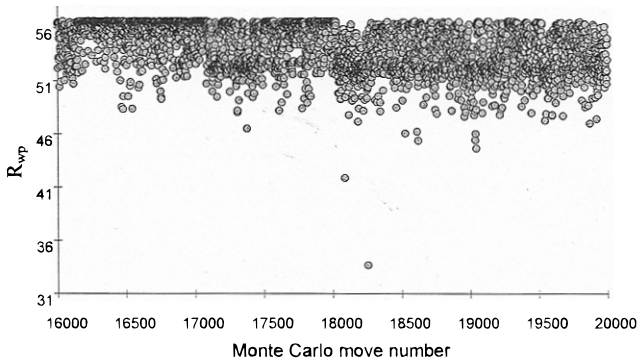

Figure 8. R_{wp} for trial structures generated in the Monte Carlo structure solution calculation for 1-methylfluorene versus the corresponding Monte Carlo move number. Only the results from the last 4000 Monte Carlo moves are shown.

fluorenyl group can fit the correct structure in two equivalent ways, whereas a structural fragment comprising the fluorenyl group plus the methyl carbon atom can fit the correct structure in only one way]. The structural fragment was subjected to simultaneous translation and rotation for a total of 20 000 Monte Carlo moves, with each translation followed by 25 rotations about the center of the five-membered ring. In each translation, the random displacement in the position of the structural fragment was constrained such that the maximum allowed change in each of the *x*, *y*, and *z* coordinates (in an orthogonal reference frame) was 0.8 Å, and in each random rotation of the structural fragment the maximum allowed angles of rotation about each of three mutually perpendicular axes was ±90°. The parameter *S* was taken as 1.8, giving 41.5% acceptance of trial structures. As the data at high diffraction angle are very weak (and therefore unlikely to give good discrimination between the correct structure and incorrect structures), R_{wp} was calculated only over the restricted range $5° < 2\theta < 55°$ in the Monte Carlo calculation. The typical value of R_{wp} for "incorrect" structures was ca. 50−56%, the value of R_{wp} for the best structure (i.e., with lowest R_{wp}) was 33.7% (Monte Carlo move number 18 251 (Figure 8)), and no other unrelated structure had R_{wp} below 43%. The distribution of R_{wp} values for the trial structures generated in the last 4000 Monte Carlo moves is shown in Figure 8. There is a clear discrimination in R_{wp} between the best structure solution and other positions of the structural fragment. The best structure solution was then taken as the starting point for difference Fourier analysis (which located the C atom of the methyl group), and the complete structure was then refined, with the application of geometric restraints, by the Rietveld refinement technique. The H atoms of the fluorenyl group were added in positions consistent with standard geometry, whereas the H atoms of the methyl group were not introduced into the model. For the C atoms, a common isotropic atomic displacement parameter was refined; for the H atoms, a common isotropic atomic displacement parameter was also used but not refined. Due to the presence of a large asymmetric peak at $2\theta = 9.07°$ in the powder diffractogram, the final Rietveld refinement was carried out over the data range $10° < 2\theta < 85°$, giving agreement factors $R_{wp} = 5.88\%$, $R_p = 4.35\%$, $R_F = 10.47\%$, $R_B = 8.55\%$, and $\chi^2 = 2.23$ for 80 variables distributed over 3791 profile points (697 reflections). The experimental and calculated X-ray

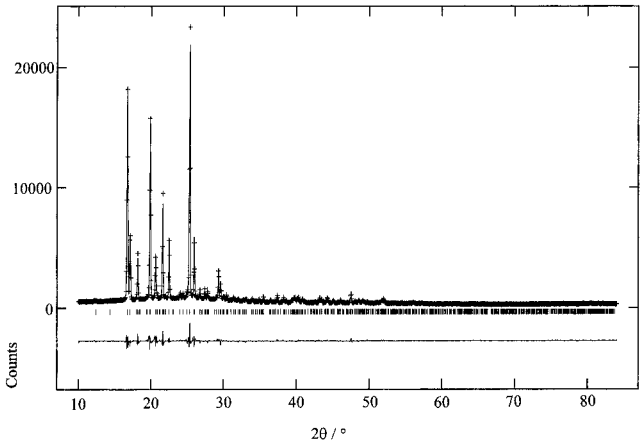

Figure 9. Experimental (+), calculated (solid line), and difference (bottom) powder diffraction profiles for the Rietveld refinement of 1-methylfluorene. Reflection positions are marked. The calculated powder diffraction profile is for the final refined crystal structure, details of which are given in Table 3.

Table 3. Final Refined Atomic Coordinates (First Line) for 1-Methylfluorene Obtained from Rietveld Refinement and the Corresponding Coordinates (Second Line) Obtained from the Monte Carlo Structure Solution Calculation[a]

atom	*x*/*a*	*y*/*b*	*z*/*c*	Δ/Å
C1	0.198(1)	1.143(2)	−0.035(1)	
	0.202	1.088	−0.009	0.52
C2	0.271(1)	0.983(2)	−0.044(1)	
	0.280	0.934	−0.001	0.74
C3	0.299(1)	0.810(2)	0.037(1)	
	0.290	0.772	0.083	0.76
C4	0.239(1)	0.763(2)	0.119(1)	
	0.223	0.761	0.158	0.67
C5	0.165(1)	0.918(2)	0.125(1)	
	0.146	0.914	0.149	0.46
C6	0.097(1)	0.928(2)	0.209(1)	
	0.067	0.942	0.217	0.43
C7	0.086(1)	0.783(2)	0.297(1)	
	0.044	0.820	0.311	0.56
C8	0.013(1)	0.831(2)	0.363(1)	
	−0.037	0.879	0.361	0.63
C9	−0.047(1)	1.020(2)	0.336(1)	
	−0.095	1.059	0.317	0.60
C10	−0.039(1)	1.159(2)	0.244(1)	
	−0.072	1.178	0.224	0.44
C11	0.035(1)	1.113(2)	0.183(1)	
	0.009	1.117	0.174	0.28
C12	0.063(1)	1.242(1)	0.084(1)	
	0.048	1.219	0.075	0.27
C13	0.143(1)	1.100(2)	0.050(1)	
	0.135	1.075	0.067	0.42
C14	0.175(1)	1.337(2)	−0.116(1)	

[a] For each atom, Δ represents the distance between the final refined position and the position obtained from the Monte Carlo calculation. The methyl carbon atom (omitted from the structural fragment used in the Monte Carlo calculation) is C14. $P2_1/n$; $a = 14.2973(5)$ Å, $b = 5.7011(2)$ Å, $c = 12.3733(5)$ Å, $\beta = 95.106(2)°$.

powder diffraction patterns, and the corresponding difference profile, are shown in Figure 9. All bond lengths and bond angles in the final refined structure are within acceptable limits consistent with the precision of the data. It should be noted that the quality of the profile fit and the molecular geometry were improved significantly by including the H atoms in the refinement.

In Table 3 and Figure 10, the optimum position of the structural fragment found in the Monte Carlo calculation is compared with the positions of the non-hydrogen atoms in the final refined crystal structure.

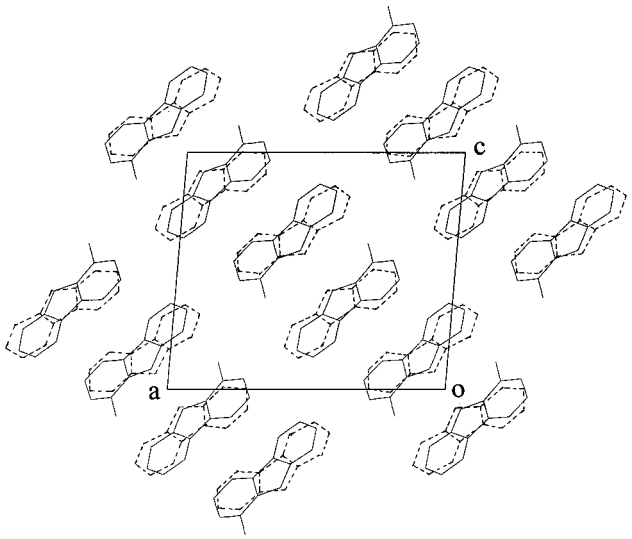

Figure 10. View along the crystallographic *b* axis of the non-hydrogen atoms in the final refined crystal structure (solid lines) of 1-methylfluorene. The best position of the structural fragment obtained from the Monte Carlo structure solution calculation (dotted lines) is also shown for comparison.

It is clear that the Monte Carlo calculation has successfully located, and discriminated, a position of the structural fragment close to its true position in the crystal structure.

6. Structure Refinement

6.1. Difference Fourier Synthesis. In favorable cases, the positions of all the atoms in the asymmetric unit may be determined at the structure solution stage, although generally only a partial structural model is obtained. In such cases, the positions of the "missing" atoms can usually be found by difference Fourier synthesis:

$$\Delta\rho(\boldsymbol{r}) = (1/V)\sum_{\mathbf{h}}(|F_o(\boldsymbol{h})| - |F_c(\boldsymbol{h})|)\exp[i\alpha_c(\boldsymbol{h}) - 2\pi i\boldsymbol{h}\cdot\boldsymbol{r}] \quad (5)$$

where $|F_o(\boldsymbol{h})|$ denotes the observed structure factor amplitude for reflection $\boldsymbol{h}$ and $|F_c(\boldsymbol{h})|$ and $\alpha_c(\boldsymbol{h})$ denote the structure factor amplitude and phase for reflection $\boldsymbol{h}$ calculated from the structural model. The difference Fourier map $\Delta\rho(\boldsymbol{r})$ reveals the discrepancies, in direct space, between the experimental powder diffraction data and the powder diffraction data calculated for the structural model. The difference Fourier map has peaks at positions in which the structural model has a deficit of electron density (e.g., when an atom is missing from the model), and troughs at positions in which the structural model has an excess of electron density (e.g., an incorrectly placed atom or an incorrectly assigned atom type). As specified above, the difference Fourier calculation considers integrated intensities extracted from the powder diffraction pattern, and peak overlap may give rise to problems and limitations similar to those encountered in traditional techniques for structure solution.

The success of the difference Fourier method depends on how much of the complete structure is represented by the partial structural model used in the difference Fourier synthesis. From experience, it is apparent that structures not containing a dominant X-ray scatterer can be completed readily by difference Fourier methods provided at least 50% of the total electron density is located correctly in the partial structural model. A smaller percentage may be sufficient if the partial structural model contains a dominant X-ray scatterer.

6.2. Rietveld Refinement Technique. In Rietveld refinement[1,113,114] of a crystal structure from powder diffraction data, every point in a digitized powder diffraction profile is considered as an intensity measurement. The powder diffraction profile for the structural model is calculated using the following information: (1) lattice parameters (to determine peak positions); (2) atomic positions and atomic displacement parameters (to determine peak intensities); (3) 2θ-dependent analytical functions to describe the peak shapes and peak widths; (4) a description of the background intensity. The shape of a peak in a powder diffractogram depends on features of both the instrument and the sample, and different types of peak shape function are appropriate under different circumstances. The most widely used peak shape function for X-ray powder diffraction data is the pseudo-Voigt function,[115] which allows flexible variation of the Gaussian and Lorentzian character of the peak shape. Analytical functions are also used to describe the 2θ dependence of the peak width, and the importance of having functions that give good representations of the 2θ dependence for different methods of powder diffraction data collection is emphasized (see, for example, refs 113 and 116).

In Rietveld refinement, the calculated powder diffraction pattern is compared, point by point, with the experimental powder diffraction pattern, and selected parameters defining the structural model and describing the profile are adjusted by least-squares methods to give the best fit. Several criteria can be used[113,115] to assess the agreement between the experimental and calculated powder diffraction patterns. Definitions of the most commonly used agreement factors are

$$R_{wp} = 100 \times \left(\frac{\sum_i w_i(y_i(\text{obs}) - y_i(\text{calc}))^2}{\sum_i w_i(y_i(\text{obs}))^2}\right)^{1/2} \quad (6)$$

$$R_p = 100 \times \frac{\sum_i |y_i(\text{obs}) - y_i(\text{calc})|}{\sum_i |y_i(\text{obs})|} \quad (7)$$

$$R_F = 100 \times \frac{\sum_k |(I_k(\text{obs}))^{1/2} - (I_k(\text{calc}))^{1/2}|}{\sum_k (I_k(\text{obs}))^{1/2}} \quad (8)$$

$$R_B = 100 \times \frac{\sum_k |I_k(\text{obs}) - I_k(\text{calc})|}{\sum_k |I_k(\text{obs})|} \quad (9)$$

$$R_e = 100 \times \left(\frac{N - P}{\sum_i w_i (y_i(\text{obs}))^2} \right)^{1/2} \quad (10)$$

$$\chi^2 = (R_{wp}/R_e)^2 \quad (11)$$

where y_i(obs) is the intensity of the ith data point in the experimental powder diffraction profile, y_i(calc) is the intensity of the ith data point in the calculated powder diffraction profile, w_i is a weighting factor for the ith data point, I_k(obs) is the intensity of the kth Bragg reflection determined from the experimental powder diffraction profile, I_k(calc) is the intensity of the kth Bragg reflection determined from the calculated powder diffraction profile, N is the number of data points in the experimental powder diffraction profile and P is the number of parameters in the refinement.

Several programs are available for carrying out Rietveld refinement, including GSAS,[28] FULLPROF,[29] PROFIL,[31] DBW,[117] and RIETAN.[118]

For Rietveld refinement to be successful, the initial structural model (obtained from the structure solution calculation) must be a sufficiently good representation of the correct crystal structure. In our experience, atoms located in the structure solution to within ca. 1 Å of their correct position will generally shift readily to their correct position upon Rietveld refinement (provided the model contains a significant amount of the complete structure). If the initial structural model is not a sufficiently good representation of the correct structure, the refinement may become trapped in a false least-squares minimum generating an incorrect structure, or the refinement may "explode" with catastrophic shifts in the parameters defining the structural model. In such cases, the refinement can often be stabilized by introducing geometric restraints (soft constraints) based on structural knowledge; these bias the refinement to shift in the direction of structurally reasonable results, and excessive shifts in the atomic positions are hindered. In general, the additional information introduced with the use of restraints allows a greater number of parameters to be refined than would be possible in unrestrained refinement from the same experimental data and generally leads to improved results in the case of structure refinement using powder diffraction data of poor quality.

Restrained Rietveld refinement has also been used as a tool in the structure solution stage of crystal structure determination from neutron powder diffraction data[119] and in combination with minimization of intermolecular potential energy.[120]

7. Experimental Considerations

Before structure solution from powder diffraction data can be attempted, it is essential that the lattice parameters are known. Although in some cases the lattice parameters may already be known independently of the powder diffraction data (e.g., from electron diffraction), they are usually determined directly from the powder diffraction pattern using the autoindexing procedures discussed in section 4.1. These autoindexing calculations have a high chance of success provided the data quality is high and provided the sample is a single phase. However, such calculations will almost certainly fail if the sample contains (but is not known to contain) a crystalline impurity or a second phase of the same compound. If the identity of an impurity or second phase is known, the peaks arising from this phase can be excluded from the powder diffractogram before carrying out the autoindexing calculation. Indexing procedures can also fail if there is significant zero-point error in the detector or poor definition of the peak positions (e.g., due to poor sample crystallinity or poor instrumental resolution).

Assuming that the lattice parameters have been determined, structure solution will succeed only if the powder diffractogram contains reliable information on the intrinsic relative intensities of the diffraction maxima; this relies on there being no "preferred orientation" in the sample. Preferred orientation arises when the crystallites in the polycrystalline sample are oriented preferentially in certain directions and can be particularly severe when the crystal morphology is significantly anisotropic (e.g., long needles or flat plates). The resulting nonrandom distribution of crystallite orientations in the sample leads to the measured relative peak intensities differing (often markedly) from the intrinsic relative diffraction intensities, severely limiting the ability to determine reliable structural information from the powder diffraction pattern. The existence of preferred orientation in a polycrystalline sample can often be detected by measuring the powder diffraction data for the same sample in different types of sample holder (e.g., capillary versus flat sample) or for different measurement geometries (e.g., reflection versus transmission). If there are differences in the relative peak intensities in the diffractograms recorded in these different ways, preferred orientation is clearly a problem. Often the effects of preferred orientation are less severe for a sample loaded in a capillary than for other types of sample holder, and it has also been suggested[121] that end-loading sample holders reduce the extent of preferred orientation. Other experimental approaches for minimizing the degree of preferred orientation include mixing the sample with an amorphous material, or appropriate grinding to induce a crystal morphology that is as isotropic as possible.

Even if the effects of preferred orientation cannot be eliminated from the experimental powder diffractogram, corrections for preferred orientation can be made retrospectively once a sufficiently good structural model is known (allowing the discrepancies between the measured relative intensities and the intrinsic relative intensities to be modeled mathematically). As these corrections can, in general, be applied only in refinement of a complete structural model,[122] attempted structure solution from powder diffraction data affected significantly by preferred orientation is usually unsuccessful. However, methods are currently being developed[123,124] for the early detection of preferred orientation by mathematical means and the subsequent application of corrections based on statistical analysis of the intensities of reflections determined from pattern decomposition.

Structure solution methods based on the use of known fragments rather than the direct extraction of intensity data from the powder diffraction pattern may prove to be more robust than the traditional methods for struc-

ture solution in allowing a valid structure solution to be obtained from data that is subject to some degree of preferred orientation. This has recently been illustrated, in the case of the Monte Carlo technique, by the structure solution of benzoic acid from powder diffraction data known to be influenced by preferred orientation.[125] Attempts to solve the structure using direct methods were unsuccessful, whereas the structure solution obtained from the Monte Carlo calculation refined readily, with the use of a preferred orientation parameter, to the known crystal structure of this material.

A detailed general account of experimental factors relating to the measurement of powder diffraction data has been given in a recent review.[8]

8. Examples of Crystal Structure Solution from Powder Diffraction Data

8.1. Framework Structures and Nonmolecular Solids. The majority of crystal structures that have been solved from powder diffraction data are framework structures and nonmolecular ionic solids. In such cases, Patterson techniques are often used, as location of the dominant scatterers in the structure often provides a sufficiently good structural model for successful completion by difference Fourier and Rietveld refinement techniques. Representative examples include $ZrKH(PO_4)_2$[39] and $Nd(OH)_2NO_3 \cdot H_2O$[41] (solved from laboratory X-ray powder diffraction data by location of the Zr and Nd positions respectively), $MnPO_4 \cdot H_2O$[42] (solved from synchrotron X-ray powder diffraction data by location of the Mn atom) and α-$CrPO_4$[40] (solved from synchrotron X-ray powder diffraction data by location of the Cr and P atoms).

However, sometimes it is necessary to determine the positions of a greater number of atoms in the structure solution stage (particularly for structures with a larger number of atoms in the asymmetric unit), and the direct methods technique has been applied successfully in many cases of this type. Examples include the following:

(1) From laboratory X-ray powder diffraction data: β-$VO(HPO_4) \cdot 2H_2O$[64] (structure solution located two V atoms, two P atoms, and ten O atoms of the 18 atoms in the asymmetric unit); β-Ba_3AlF_9[67] (structure solution located seven Ba atoms of the 29 atoms in the asymmetric unit).

(2) From synchrotron X-ray powder diffraction data: $LaMo_5O_8$[126] (structure solution located all six heavy atoms); sigma-2 clathrasil[127] (structure solution located all four Si atoms and four O atoms out of the 11 framework atoms); $Ga_2(HPO_3)_3 \cdot 4H_2O$[66] (structure solution located two Ga atoms of the 29 atoms in the asymmetric unit).

In all these cases, the partial structures were completed successfully using difference Fourier and Rietveld refinement techniques.

The most complex structures (in terms of number of atoms in the asymmetric unit) to be determined from powder diffraction data have been solved using a combination of synchrotron X-ray data together with either laboratory X-ray data or neutron data. For example, the crystal structure of $La_3Ti_5Al_{15}O_{37}$[17] was solved using synchrotron X-ray data and neutron data. Direct methods located the three La atoms and two Ti atoms and subsequent difference Fourier synthesis revealed 9 more metal atoms and 27 O atoms from the synchrotron X-ray data. The 19 remaining atoms were then located by difference Fourier techniques applied to the neutron data. To further improve the quality of the refinement, a neutron powder diffraction pattern was collected at longer wavelength (improving the resolution at high diffraction angle) and used in a joint refinement with the X-ray diffraction data.

The importance of extracting reliable intensity information from the powder diffraction pattern for use in direct methods structure solution calculations is illustrated by the reported structure determination[34] of the silicoaluminophosphate material SAPO-40. In this work, the use of the FIPS procedure to determine intensity information for overlapping peaks was found to be essential in order for subsequent direct methods calculations to produce a successful structure solution. The structure solution comprised the four T atoms (i.e., the Al, Si, and P atoms, which were not distinguished) and five of the ten O atoms in the asymmetric unit. The knowledge of the framework topology, established from the positions of the four T atoms, allowed the positions of the five remaining O atoms to be deduced readily.

8.2. Molecular Crystals. Although a considerable number of nonmolecular and framework crystal structures have been determined from X-ray powder diffraction data, substantially less has been achieved in the field of molecular crystallography. In part, the challenges encountered in crystal structure solution are greater in the case of molecular crystals. Molecular crystals tend to have low symmetry, leading to substantial overlap of peaks in the powder diffractogram. Furthermore, for organic molecular crystals, the majority of the atoms in the structure are weak X-ray scatterers, resulting in little significant intensity at high diffraction angles.

8.2.1. Organometallics and Organic Compounds Containing Elements Heavier Than Oxygen. If the structure contains a limited number of strong X-ray scatterers, their positions can generally be determined using the Patterson method, and the structure can then be completed using difference Fourier techniques[44] or by a combination of difference Fourier techniques and positioning additional atoms on the basis of known geometry.[128,129] However, if the strong scatterers do not constitute a sufficiently large fraction of the complete structure for subsequent refinement to be successful, other methods of structure solution must be used. Problems can also arise for structures that contain a very strong X-ray scatterer, for which it may be difficult to establish reliably the positions of the other atoms in the structure from X-ray diffraction data.

The first structure solution of a molecular crystal from powder diffraction data by direct methods was for the previously known structure of cimetidine,[130] using synchrotron X-ray powder diffraction data. In this case, the whole structure was identified from the E-map obtained in the direct methods calculation. Recently, this approach has been used to determine the previously unknown crystal structure of chlorothiazide[131] at 130 K; all 17 non-hydrogen atom positions were obtained from the direct methods structure solution calculation. The direct methods approach has also been applied to solve unknown molecular crystal structures from pow-

der diffraction data recorded using laboratory X-ray sources.[44,68,71] In these cases, the direct methods procedures yielded only partial structure solutions that were completed by difference Fourier and Rietveld refinement techniques. The combined maximum entropy and likelihood method has also been used.[89,132]

Many molecules contain fragments of well-defined geometry, and several structures have been solved using methods based on movement of these fragments within the unit cell, actively exploiting the knowledge of molecular geometry in the structure solution process. A program combining both Patterson and direct methods has been used to locate all the non-hydrogen atoms in the structure of an anhydrous copper(II) 8-hydroxyquinolinato complex[52] by location of the molecular model around the fixed heavy atom position. As discussed in section 5.4.1, the Monte Carlo approach has been used to determine a number of molecular crystal structures[103,105] in which the structural fragment comprised only a fraction of the atoms in the asymmetric unit, with the structures then completed using difference Fourier and Rietveld refinement techniques. One of these structures—*m*-chloro-*trans*-cinnamic acid—represents an interesting example of structure solution in which the dominant X-ray scatterer was actually omitted from the structure solution calculation; the structural fragment used in the Monte Carlo calculation comprised all C and O atoms of the *trans*-cinnamic acid system, but with the Cl atom omitted (inclusion of the Cl atom would have required an internal degree of freedom to be considered in the Monte Carlo calculation). The Cl atom was found subsequently by difference Fourier techniques. The simulated annealing structure solution method has been used[104] in the structure determination of $Li_3[Co(CN)_5]\cdot 2DMF$ from synchrotron X-ray powder diffraction data, with the $Co(CN)_5$ moiety and two DMF molecules located in the structure solution calculation.

A three-dimensional search procedure (P-RISCON[133]), involving comparison of calculated and observed integrated intensities, has also been applied to determine several crystal structures, including $[HgRu(CO)_4]_4$[134] (by location and orientation of the Hg_4Ru_4 fragment) and polymeric silver imidazolate.[135]

8.2.2. "Equal-Atom" Organic Crystals. The problems encountered in solving "equal atom" structures (e.g., organic compounds containing no atom heavier than oxygen) are particularly severe. For these structures, our experience has shown that a substantial proportion (at least 50%) of the non-hydrogen atoms must be located correctly in the structure solution calculation in order for subsequent structure refinement to be successful. In addition, the lack of prominent peaks in electron density maps produced during structure solution of "equal atom" structures often makes the identification of atomic positions difficult and unreliable. To our knowledge, only one previously unknown "equal atom" organic structure (formylurea[69]) has been solved from X-ray powder diffraction data using direct methods. All other structures of this type that have been solved from powder diffraction data contain a well-defined fragment of known geometry (usually a planar fragment constituting a significant proportion of the scattering matter). The approaches used to solve these structures have included calculation of the orientation and translation vector of the fragment (POSIT[136]), a combined Patterson and trial-and-error method,[137] a method based on the use of atom−atom potentials,[138] and Patterson fragment search methods (first demonstrated for a number of previously known organic structures,[48,49] and recently applied to determine the crystal structure of the 2-(3,4-dihydroxyphenyl)-α-nitronyl nitroxide radical[51]). More recently, the Monte Carlo method has been applied to solve the crystal structures of *p*-methoxybenzoic acid,[106] 1-methylfluorene[107] and fluorescein.[112] A simulated annealing approach has also been applied successfully to solve the known crystal structure of benzene from simulated X-ray powder diffraction data.[102]

9. Future Prospects

The above discussion has demonstrated the feasibility of solving crystal structures from powder diffraction data and has illustrated the scope and limitations of the methods that are currently available for this purpose. All of the methods described have a significant role to play in the future, and it is important to establish precisely the circumstances under which each method represents the best approach for crystal structure solution. It is only when this knowledge has been established that it will be possible to decide, a priori, which method should be chosen for any particular class of structural problem or for any particular set of powder diffraction data.

Although significant progress has been made in recent years in the application of the methods for structure solution described in this review, there is considerable scope for the development of new methods for attacking the structure solution stage of the structure determination process. One approach that may prove to be particularly powerful is to combine the structure solution methods described above with computer simulation techniques that allow the prediction of crystal structures. With the increasing availability of reliable potential energy parametrizations for many types of solid, and progress in the development of computational methods for crystal structure prediction, it is likely that a combined approach will emerge in the near future as a powerful technique for crystal structure solution from powder diffraction data. The rapidly evolving direct space methods for crystal structure solution from powder diffraction data hold particular promise as a key component of such a combined approach.

In summary, recent developments in methodology for structure solution and other stages of the structure determination process, together with continuing developments in instrumentation for recording powder diffraction data of improved quality, promise an optimistic outlook for the field of crystal structure determination from powder diffraction data, and we confidently predict that the future will yield considerable new information on a wide range of important materials that have hitherto defied structural characterization.

Acknowledgment. We are grateful to Dr. Benson Kariuki and Dr. Phil Lightfoot for many useful discussions in connection with this field of research, and to E.P.S.R.C., the Nuffield Foundation and Ciba Geigy Ltd. for financial support. We thank Dr. Chris Gilmore and Dr. Kenneth Shankland for permission to report un-

published work, and Professor Peter Bruce for his involvement in the work described in ref 95.

References

(1) Rietveld, H. M. *J. Appl. Crystallogr.* **1969**, *2*, 65.
(2) Christensen, A. N.; Lehmann, M. S.; Nielsen, M. *Aust. J. Phys.* **1985**, *38*, 497.
(3) Cheetham, A. K.; Wilkinson, A. P. *J. Phys. Chem. Solids* **1991**, *52*, 1199.
(4) McCusker, L. B. *Acta Crystallogr.* **1991**, *A47*, 297.
(5) Cheetham, A. K.; Wilkinson, A. P. *Angew. Chem., Int. Ed. Engl.* **1992**, *31*, 1557.
(6) Rudolf, P. *Mater. Chem. Phys.* **1993**, *35*, 267.
(7) Cheetham, A. K. In *The Rietveld Method*; IUCr; Oxford University Press: Oxford, UK; Young, R. A., Ed.; 1993; pp 276−292.
(8) Langford, J. I.; Louër, D. *Rep. Progr. Phys.* **1996**, *59*, 131.
(9) Hill, R. J.; Cranswick, L. M. D. *J. Appl. Crystallogr.* **1994**, *27*, 807.
(10) Cheetham, A. K.; David, W. I. F.; Eddy, M. M.; Jakeman, R. J. B.; Johnson, M. W.; Torardi, C. C. *Nature* **1986**, *320*, 46.
(11) Jouanneaux, A.; Fitch, A. N.; Cockcroft, J. K. *Mol. Phys.* **1992**, *1*, 45.
(12) Delaplane, R. G.; David, W. I. F.; Ibberson, R. M.; Wilson, C. C. *Chem. Phys. Lett.* **1993**, *201*, 75.
(13) Vogt, T.; Fitch, A. N.; Cockroft, J. K. *Science* **1994**, *263*, 1265.
(14) Ibberson, R. M.; Prager, M. *Acta Crystallogr.* **1995**, *B51*, 71.
(15) Tremayne, M.; Lightfoot, P.; Mehta, M. A.; Bruce, P. G.; Harris, K. D. M.; Shankland, K.; Gilmore, C. J.; Bricogne, G. *J. Solid State Chem.* **1992**, *100*, 191.
(16) Abrahams, I.; Lightfoot, P.; Bruce, P. G. *J. Solid State Chem.* **1993**, *104*, 397.
(17) Morris, R. E.; Owen, J. J.; Stalick, J. K.; Cheetham, A. K. *J. Solid State Chem.* **1994**, *111*, 52.
(18) Louër, M.; Brochu, R.; Louër, D.; Arsalane, S.; Ziyad, M. *Acta Crystallogr.* **1995**, *B51*, 908.
(19) Visser, J. W. *J. Appl. Crystallogr.* **1969**, *2*, 89.
(20) Werner, P.-E.; Eriksson, L.; Westdahl, M. *J. Appl. Crystallogr.* **1985**, *18*, 367.
(21) Boultif, A.; Louër, D. *J. Appl. Crystallogr.* **1991**, *24*, 987.
(22) Shirley, R. *Data Accuracy for Powder Indexing*; Natl. Bur. Stand. (US) Spec. Publ. No. 567, 1980; p 361.
(23) De Wolff, P. M. *J. Appl. Crystallogr.* **1968**, *1*, 108.
(24) Smith, G. S.; Snyder, R. L. *J. Appl. Crystallogr.* **1979**, *12*, 60.
(25) Pawley, G. S. *J. Appl. Crystallogr.* **1981**, *14*, 357.
(26) Toraya, H. *J. Appl. Crystallogr.* **1986**, *19*, 440.
(27) Le Bail, A.; Duroy, H.; Fourquet, J. L. *Mater. Res. Bull.* **1988**, *23*, 447.
(28) Larson, A. C.; Von Dreele, R. B. Los Alamos Laboratory Report No. LA-UR-86-748, 1987.
(29) Rodriguez-Carvajal, J. In *Collected Abstracts of Powder Diffraction Meeting*; Toulouse, France, July, 1990; p 127.
(30) Jansen, J.; Peschar, R.; Schenk, H. *J. Appl. Crystallogr.* **1992**, *25*, 231.
(31) Cockcroft, J. K. PROFIL, Version 5.17, Department of Crystallography, Birkbeck College, U.K., 1994.
(32) Altomare, A.; Burla, M. C.; Cascarano, G.; Guagliardi, A.; Moliterni, A. G. G.; Polidori, G. *J. Appl. Crystallogr.* **1995**, *28*, 842.
(33) Jansen, J.; Peschar, R.; Schenk, H. *J. Appl. Crystallogr.* **1992**, *25*, 237.
(34) Estermann, M. A.; McCusker, L. B.; Baerlocher, C. *J. Appl. Crystallogr.* **1992**, *25*, 539.
(35) David, W. I. F. *J. Appl. Crystallogr.* **1987**, *20*, 316.
(36) David, W. I. F. *Nature* **1990**, *346*, 731.
(37) Sivia, D. S.; David, W. I. F. *Acta Crystallogr.* **1994**, *A50*, 703.
(38) Patterson, A. L. *Phys. Rev.* **1934**, *46*, 372.
(39) Clearfield, A.; McCusker, L. B.; Rudolf, P. R. *Inorg. Chem.* **1984**, *23*, 4679.
(40) Attfield, J. P.; Sleight, A. W.; Cheetham, A. K. *Nature* **1986**, *322*, 620.
(41) Louër, D.; Louër, M. *J. Solid State Chem.* **1987**, *68*, 292.
(42) Lightfoot, P.; Cheetham, A. K.; Sleight, A. W. *Inorg. Chem.* **1987**, *26*, 3544.
(43) Benard, P.; Louër, M.; Louër, D. *J. Solid State Chem.* **1991**, *94*, 27.
(44) Lightfoot, P.; Glidewell, C.; Bruce, P. G. *J. Mater. Chem.* **1992**, *2*, 361.
(45) Wilson, C. C.; Tollin, P. *J. Appl. Crystallogr.* **1986**, *19*, 411.
(46) Rius, J.; Miravitlles, C. *J. Appl. Crystallogr.* **1987**, *20*, 261.
(47) Egert, E.; Sheldrick, G. M. *Acta Crystallogr.* **1985**, *A41*, 262.
(48) Wilson, C. C. *Acta Crystallogr.* **1989**, *A45*, 833.
(49) Wilson, C. C.; Wadsworth, J. W. *Acta Crystallogr.* **1990**, *A46*, 258.
(50) Rius, J.; Miravitlles, C. *J. Appl. Crystallogr.* **1988**, *21*, 224.
(51) Cirujeda, J.; Ochando, L. E.; Amigo, J. M.; Rovira, C.; Rius, J.; Veciana, J. *Angew. Chem., Int. Ed. Engl.* **1995**, *34*, 55.
(52) Petit, S.; Coquerel, G.; Perez, G.; Louër, D.; Louër, M. *Chem. Mater.* **1994**, *6*, 116.
(53) Woolfson, M. M. *Acta Crystallogr.* **1987**, *A43*, 593.
(54) Ladd, M. F. C., Palmer, R. A., Eds. *Theory and Practice of Direct Methods in Crystallography*; Plenum Press: New York, 1980.
(55) Main, P. MULTAN84, University of York, UK, 1984.
(56) Sheldrick, G. M. *Crystallographic Computing 3*; Sheldrick, G. M., Ed.; Oxford University Press: Oxford, UK, 1985; p 175.
(57) Gilmore, C. J. *J. Appl. Crystallogr.* **1984**, *12*, 42.
(58) Gilmore, C. J.; Brown, S. R. *J. Appl. Crystallogr.* **1988**, *21*, 571.
(59) Burla, M. C.; Camalli, M.; Cascarano, G.; Giacovazzo, C.; Polidori, G.; Spagna, R.; Viterbo, D. *J. Appl. Crystallogr.* **1989**, *22*, 389.
(60) Altomare, A.; Cascarano, G.; Giacovazzo, C.; Guagliardi, A.; Burla, M. C.; Polidori, G.; Camalli, M. *J. Appl. Crystallogr.* **1994**, *27*, 435.
(61) Peschar, R. SIMPEL, *Molecular Structure Solution Procedures*; Enraf-Nonius: Delft, 1990; Vol. 3, p 59.
(62) Cascarano, G.; Favia, L.; Giacovazzo, C. *J. Appl. Crystallogr.* **1992**, *25*, 310.
(63) Jansen, J.; Peschar, R.; Schenk, H. *Z. Kristallogr.* **1993**, *206*, 33.
(64) Le Bail, A.; Ferey, G.; Amoros, P.; Beltran-Porter, D.; Villeneuve, G. *J. Solid State Chem.* **1989**, *79*, 169.
(65) Louër, D.; Louër, M.; Touboul, M. *J. Appl. Crystallogr.* **1992**, *25*, 617.
(66) Morris, R. E.; Harrison, W. T. A.; Nicol, J. M.; Wilkinson, A. P.; Cheetham, A. K. *Nature* **1992**, *359*, 519.
(67) Le Bail, A. *J. Solid State Chem.* **1993**, *103*, 287.
(68) Lasocha, W.; Jansen, J.; Schenk, H. *J. Solid State Chem.* **1995**, *117*, 103.
(69) Lightfoot, P.; Tremayne, M.; Harris, K. D. M.; Bruce, P. G. *J. Chem. Soc., Chem. Commun.* **1992**, 1012.
(70) Williams, J. H.; Cockcroft, J. K.; Fitch, A. N. *Angew. Chem., Int. Ed. Engl.* **1992**, *31*, 1655.
(71) Petit, S.; Coquerel, G.; Perez, G.; Louër, D.; Louër, M. *New J. Chem.* **1993**, *17*, 187.
(72) Colapietro, M.; Domenicano, A. *Acta Crystallogr.* **1978**, *B34*, 3277.
(73) Gull, S. F.; Daniell, G. J. *Nature* **1978**, *272*, 686.
(74) Buck, B., Macaulay, V. A., Eds. *Maximum Entropy in Action*; Oxford University Press: Oxford, UK, 1992.
(75) Gilmore, C. J. *Acta Crystallogr.* **1996**, *A52*, 561.
(76) Wilkins, S. W.; Varghese, J. N.; Lehmann, M. S. *Acta Crystallogr.* **1983**, *A39*, 47.
(77) Livesey, A. K.; Skilling, J. *Acta Crystallogr.* **1985**, *A41*, 113.
(78) Sakata, M.; Mori, R.; Kumazawa, S.; Takata, M.; Toraya, H. *J. Appl. Crystallogr.* **1990**, *23*, 526.
(79) Narayan, R.; Nityananda, R. *Acta Crystallogr.* **1982**, *A38*, 122.
(80) Britten, P. L.; Collins, D. M. *Acta Crystallogr.* **1982**, *A38*, 129.
(81) Piro, O. E. *Acta Crystallogr.* **1983**, *A39*, 61.
(82) Bricogne, G. *Acta Crystallogr.* **1984**, *A40*, 410.
(83) Bricogne, G.; Gilmore, C. J. *Acta Crystallogr.* **1990**, *A46*, 284.
(84) Gilmore, C. J.; Bricogne, G.; Bannister, C. *Acta Crystallogr.* **1990**, *A46*, 297.
(85) Gilmore, C. J.; Henderson, A. N.; Bricogne, G. *Acta Crystallogr.* **1991**, *A47*, 842.
(86) Dong, W.; Baird, T.; Fryer, J. R.; Gilmore, C. J.; MacNicol, D. D.; Bricogne, G.; Smith, D. J.; O'Keefe, M. A.; Hovmoller, S. *Nature* **1992**, *355*, 605.
(87) Voigtmartin, I. G.; Yan, D. H.; Yakimansky, A.; Schollmeyer, D.; Gilmore, C. J.; Bricogne, G. *Acta Crystallogr.* **1995**, *A51*, 849.
(88) Gilmore, C. J.; Henderson, K.; Bricogne, G. *Acta Crystallogr.* **1991**, *A47*, 830.
(89) Tremayne, M.; Lightfoot, P.; Glidewell, C.; Harris, K. D. M.; Shankland, K.; Gilmore, C. J.; Bricogne, G.; Bruce, P. G. *J. Mater. Chem.* **1992**, *2*, 1301.
(90) Shankland, K.; Gilmore, C. J.; Bricogne, G.; Hashizume, H. *Acta Crystallogr.* **1993**, *A49*, 493.
(91) Gilmore, C. J.; Shankland, K.; Bricogne, G. *Proc. R. Soc. London A* **1993**, *442*, 97.
(92) Bricogne, G. *Acta Crystallogr.* **1991**, *A47*, 803.
(93) Bricogne, G. *Acta Crystallogr.* **1993**, *D49*, 37.
(94) Gilmore, C. J., personal communication.
(95) Tremayne, M. Ph.D. Thesis, University of St. Andrews, Scotland, 1995.
(96) Metropolis, K.; Ulam, S. *J. Am. Stat. Assoc.* **1949**, *44*, 335.
(97) Allen, M. P.; Tildesley, D. J. *Computer Simulation of Liquids*; Oxford University Press: Oxford, UK, 1987.
(98) Ciccotti, G.; Frenkel, D.; McDonald, I. R. *Simulation of Liquids and Solids* North-Holland: Amsterdam, 1987.
(99) Kirkpatrick, S.; Gelatt, C. D.; Vecchi, M. P. *Science* **1983**, *220*, 671.
(100) van Laarhoven, P. J. M.; Aarts, E. H. L. *Simulated Annealing: Theory and Applications*; D. Riedel Publishing: Holland, 1987.
(101) Deem, M. W.; Newsam, J. M. *Nature* **1989**, *342*, 360.
(102) Newsam, J. M.; Deem, M. W.; Freeman, C. M. *Accuracy in Powder Diffraction II: NIST Special Publication* **1992**, *846*, 80.
(103) Harris, K. D. M.; Tremayne, M.; Lightfoot, P.; Bruce, P. G. *J. Am. Chem. Soc.* **1994**, *116*, 3543.
(104) Ramprasad, D.; Pez, G. P.; Toby, B. H.; Markley, T. J.; Pearlstein, R. M. *J. Am. Chem. Soc.* **1995**, *117*, 10694.

(105) Kariuki, B. M.; Zin, D. M. S.; Tremayne, M.; Harris, K. D. M. *Chem. Mater.* **1996**, *8*, 565.
(106) Tremayne, M.; Kariuki, B. M.; Harris, K. D. M. *J. Appl. Crystallogr.* **1996**, *29*, 211.
(107) Tremayne, M.; Kariuki, B. M.; Harris, K. D. M. *J. Mater. Chem.* **1996**, *6*, 1601.
(108) McGreevy, R. L.; Pustzai, L. *Mol. Simul.* **1988**, *1*, 359.
(109) Keen, D. A.; McGreevy, R. L. *Nature* **1990**, *344*, 423.
(110) Metropolis, N.; Rosenbluth, A. W.; Rosenbluth, M. N.; Teller, A. H.; Teller, E. *J. Chem. Phys.* **1953**, *21*, 1087.
(111) Rao, M.; Pangali, C.; Berne, B. J. *Mol. Phys.* **1979**, *37*, 1773.
(112) Tremayne, M.; Kariuki, B. M.; Harris, K. D. M., manuscript submitted.
(113) Young, R. A., Ed. *The Rietveld Method*; IUCr/OUP: Oxford, 1993.
(114) Hill, R. J.; Madsen, I. C. *Powder Diffraction* **1987**, *2*, 146.
(115) Young, R. A.; Wiles, D. B. *J. Appl. Crystallogr.* **1982**, *15*, 430.
(116) Caglioti, G.; Paoletti, A.; Ricci, F. P. *Nucl. Instrum.* **1958**, *3*, 223.
(117) Wiles, D. B.; Young, R. A. *J. Appl. Crystallogr.* **1981**, *14*, 149.
(118) Izumi, F.; Asano, H.; Murata, H.; Watanabe, N. *J. Appl. Crystallogr.* **1987**, *20*, 411.
(119) David, W. I. F. ISIS Annual Report, Rutherford Appleton Laboratory, 1993; Vol. 1, p 103.
(120) Oka, K.; Okada, K.; Nukada, K. *Jpn. J. Appl. Phys.* **1992**, *31*, 2181.
(121) Nakata, K.; Takaki, Y. *Bull. Chem. Soc. Jpn.* **1987**, *60*, 1168.
(122) Dollase, W. A. *J. Appl. Crystallogr.* **1986**, *19*, 267.
(123) Altomare, A.; Cascarano, G.; Giacovazzo, C.; Guagliardi, A. *J. Appl. Crystallogr.* **1994**, *27*, 1045.
(124) Peschar, R.; Schenk, H.; Capková, P. *J. Appl. Crystallogr.* **1995**, *28*, 127.
(125) Tremayne, M.; Kariuki, B. M.; Harris, K. D. M., manuscript in preparation.
(126) Hibble, S. J.; Cheetham, A. K.; Bogle, A. R. L.; Wakerley, H. R.; Cox, D. E. *J. Am. Chem. Soc.* **1988**, *110*, 3295.
(127) McCusker, L. B. *J. Appl. Crystallogr.* **1988**, *21*, 305.
(128) Berg, J.-E.; Werner, P.-E. *Z. Kristallogr.* **1977**, *145*, 310.
(129) Poojary, M. D.; Hu, H.-L.; Campbell, F. L., III; Clearfield, A. *Acta Crystallogr.* **1993**, *B49*, 996.
(130) Cernik, R. J.; Cheetham, A. K.; Prout, C. K.; Watkin, D. J.; Wilkinson, A. P.; Willis, B. T. M. *J. Appl. Crystallogr.* **1991**, *24*, 222.
(131) Shankland, K., personal communication.
(132) Lightfoot, P.; Tremayne, M.; Harris, K. D. M.; Glidewell, C.; Shankland, K.; Gilmore, C. J.; Bruce, P. G. *Mater. Sci. Forum* **1993**, *133−136*, 207.
(133) Masciocchi, N.; Bianchi, R.; Cairati, P.; Mezza, G.; Pilati, T.; Sironi, A. *J. Appl. Crystallogr.* **1994**, *27*, 426.
(134) Masciocchi, N.; Cairati, P.; Ragaini, F.; Sironi, A. *Organometallics* **1993**, *12*, 4499.
(135) Masciocchi, N.; Moret, M.; Cairati, P.; Sironi, A.; Ardizzoia, G. A.; La Monica, G. *J. Chem. Soc., Dalton Trans.* **1995**, 1671.
(136) Reck, G.; Kretschmer, R.-G.; Kutschabsky, L.; Pritzkow, W. *Acta Crystallogr.* **1988**, *A44*, 417.
(137) Honda, K.; Goto, M.; Kurahashi, M. *Chem. Lett.* **1990**, 13.
(138) Louër, D.; Louër, M.; Dzyabchenko, V. A.; Agafonov, V.; Ceolin, R. *Acta Crystallogr.* **1995**, *B51*, 182.

CM960218D